

# A simple methodology for determining optimal print parameters for 3D bioprinting with low-viscosity bioink

Elizabeth A. Heile; Elizabeth R. Komosa; Brenda M. Ogle, PhD

## Abstract

Animal models are often used to study disease, but these models are limited because they often fail to represent human anatomy and disease-state characteristics. Recently, 3D bioprinting has been employed to construct customizable and complex cell-laden tissue structures, which have the potential to complement or replace these animal models with patient-specific anatomies and disease states. Some challenges of 3D bioprinting include the use of a low-viscosity bioink, and the imposition of shear stress on cells during extrusion. The lack of quantification and optimization of 3D printing parameters with this ink-type make the generation of high-resolution, reproducible prints difficult.

In this study, a methodology was developed to quantify both the print fidelity and resolution associated with various print parameters, which was used to select a set of optimized 3D bioprinting parameters for a gelatin methacrylate (GelMA)-based bioink. The best conditions for fidelity and resolution were a print speed of 14 mm/s at a flow rate of 1 drop/4s and a print speed of 12 mm/s at a flow rate of 1 drop/4s, and the worst condition for both the fidelity and resolution was a print speed of 10 mm/s at a flow rate of 1 drop/2s. These results will inform future work, which will optimize the resolution, fidelity, and cell viability and determine an optimal set of conditions for 3D printing a cardiac organoid.

## Introduction

3D bioprinting is a novel approach utilized by biomedical engineers to generate cell-laden organ and tissue models. The advancement of these technologies has the potential to (1) improve research by replacing animal models with patient-specific anatomies and disease states and (2) support healthcare and regenerative medicine by minimizing organ transplant waitlists, diminishing the risk of organ transplant rejection, and curing a variety of degenerative diseases. While there are many other techniques for generating 3D complex tissues, such as growing tissues on biocompatible or biomimetic scaffolds, 3D printing provides scientists with a high level of

control over the placement of cells and scaffolding and allows for large-scale construction of customizable, complex, cell-dense structures.

One limitation of 3D printing soft tissue such as cardiac tissue, however, is that most bioinks are of low viscosity and would therefore pool on the build plate instead of cooling and hardening into a 3D construct like traditional plastic filament. A variety of techniques have been attempted in order to print these soft materials, such as constructing tissues layer-by-layer through electrospinning an ellipsoidal collector and dipping it into a solution of nanofibrous scaffolds and cardiomyocytes;<sup>1</sup> however, they present

challenges including the inability to create complex or non-radially symmetrical constructs. A promising method of bioprinting, deemed freeform reversible embedding of suspended hydrogels, or FRESH, involves extruding a bioink containing a photoinitiator into a support bath of gelatin slurry made by blending (FRESH) or by coacervation (FRESHv2.0),<sup>2,3</sup> followed by crosslinking with blue light. This method has been applied to print impressive structures, such as an acellular full-sized heart model, acellular heart valves, and an electromechanically functional, chambered cardiac organoid.<sup>2,3,4,5</sup>

While the FRESH method has been used to successfully print 3D acellular and cell-laden constructs, the resolution, shape fidelity, and cell viability of various bioprinting parameters are not typically assessed quantitatively, making optimal bioprinting conditions and parameters relatively unknown. For extrusion-based bioprinting, the viscosity and variability of the ink, the density of the printed structure, the mechanism of crosslinking, the properties of the support bath, and the pressure applied to extrude the ink through the nozzle, among other factors, can all affect the fidelity and reproducibility of printed structures. The cell viability of prints can also be influenced by these parameters, particularly the pressure generated by the syringe printhead, which exposes the cells in the bioink to a shear stress when passing through the syringe and nozzle.<sup>6</sup>

The optimization of bioprinting parameters is particularly important when printing with human induced pluripotent stem cell-derived cardiomyocytes (hiPSC-CMs) to develop cardiac models because their

maturation is highly dependent on their environment. Immature cardiomyocytes exhibit different electrophysiology, metabolism, contractile function, calcium handling, morphology, and protein production than mature cardiomyocytes, which may lead to poor or inaccurate results if used in disease models and drug testing.<sup>7</sup> Improved cardiac maturation has been achieved through electrical and mechanical stimulation, biochemical approaches, growth on specific materials, or culture in 3D. With a 3D bioprinting protocol that allows for optimized cell viability, reproducibility, and resolution of cardiac organoids, more definitive results regarding CM maturity could be obtained due to decreased variability between samples.

Previously, 3D bioprinting has been applied using the FRESH method to generate complex cardiac mimics using human induced pluripotent stem cells (hiPSCs).<sup>5</sup> These cardiac mimics, named human chambered muscle pumps (hChaMPs), contain complex geometry such as chambers and large vessels, which allow for perfusion and assessment of pressure-volume relationships in the construct. Because hChaMPs contain human induced pluripotent stem cells, cardiomyocyte differentiation can be induced after printing, providing high expression of the cardiomyocyte marker cardiac troponin T. We hope to further develop the functionality of this structure by improving cardiac cell maturation and viability.

The present study proposes a methodology to optimize 3D bioprinting protocols to improve the resolution and fidelity of 3D printed structures using low-viscosity inks by varying flow rate, print speed, and infill percentage. By improving these features of

prints, progress can be made towards improving the viability, maturity, and complexity of 3D printed organoids.

## Materials and Methods

### *Preparation of Support Bath*

The support bath preparation was based on methods previously reported.<sup>3</sup> First, 105 mL DI water and 95 mL 200 proof ethanol were added to a beaker, and the beaker was placed in a water bath made in a larger beaker on a combination stirring/hot plate. The solution was warmed to 45°C while stirring at 400 rpm. Once the solution reached the desired temperature, the pH of the mixture was raised to 7 using a dropwise addition of 20 $\mu$ L 1M NaOH. Gelatin type B (4g) and gum arabic (2g) were mixed together and slowly added to the solution while continuously stirring at 400 rpm to prevent clumps from forming. The solution was mixed and held at 45°C for 10 minutes to ensure that the solids were completely dissolved. The solution was cooled quickly to 30°C, then by 1°C per minute for 20 minutes by gradual addition of ice to the water bath. The solution was then stirred for 5 minutes at 10°C.

The mixture was poured into four 50mL conical tubes and centrifuged at 200 G for 4 minutes. The supernatant was replaced with DI water, and the tube was vortexed until the solids were resuspended. The tubes of support bath were again centrifuged at 300 G for 2 minutes, the supernatant was replaced with 1x PBS, and the tube was vortexed until resuspended. The resulting mixture was stored at 4°C until the day of printing, up to 5 days.

To prepare for printing using the refrigerated support bath material, a conical tube of the support bath material was

centrifuged at 1000 G for 5 minutes, the supernatant was removed, and the support material was transferred into the wells of a 24-well plate for printing.

### *Preparation of Bioink*

To prepare the bioink, 3 mL of Glasgow Modified Essential Medium (GMEM) cell culture medium was mixed with 1 mL of 1M acetic acid in a 50 mL conical tube. The conical tube was wrapped with aluminum foil to prevent premature crosslinking from light exposure, and 20 mg of lithium phenyl-2,4,6-trimethylbenzoylphosphinate (LAP) photoinitiator and 400 mg of lyophilized, frozen gelatin methacrylate (GelMA) were added to the solution. The conical tube was vortexed and warmed in a 60°C water bath for 2 hours, vortexing for 10 seconds every 30 minutes to promote dissolution.

### *Printing Procedure*

To create the print template, a 3D model designed in Solidworks was processed using Slic3r and exported as a gcode file. A Cellink BioX 3D printer was used for printing. The printhead was set to warm to 30°C, and the print speed, printhead pressure, and needle diameter were selected. The prints were carried out in a 24-well plate using a 27-gauge, 1-inch needle. After preparing the printer settings, the bioink was warmed in the 37°C water bath, pipetted into an amber print cartridge, and inserted into the pre-warmed printhead for 10 minutes prior to printing to allow the ink to reach thermal equilibrium. The flow rate was determined by adjusting the pressure, testing the flow, and using a stopwatch to measure the time between drops. Pressures were varied to

analyze flow rates in the range of 1 drop every 2 seconds to 1 drop every 4 seconds. Once the pressure was set, the printing procedure was initiated. Between each print, the procedure was paused to change printing parameters or adjust the flow rate to test various print conditions.

After printing was complete, the ink was crosslinked by shining a 405 flashlight on the top face for 30 seconds and the bottom face for 30 seconds. The 24 well plate was then placed in a 37°C incubator for 30 minutes to melt the support bath material, the support material was removed, and the printed structures were rinsed three times with 37°C 1x PBS to remove remaining support bath. The prints were stored in PBS in the 37°C incubator for 1 day before imaging.

#### *Print Fidelity and Resolution Analysis*

A drop of PBS was placed on each print to limit movement and dehydration during imaging, and a tile scan was taken of each print on a Leica S6 D microscope. The infill line thickness, the test square length and the test square side width were each measured 3 times using ImageJ and averaged for both replicates.

## **Results**

#### *Verification of Support Bath Consistency*

The support bath particles were resuspended and diluted in cold PBS to prevent undesired gelation and stored in a 4°C

refrigerator before use. In order to ensure that the support bath storage length did not affect the particle size or shape, images were taken of the support bath material on day 0, 1, 2, and 5, and the particles were measured (Figure 1). Over the course of 31 days, the measured particle size stayed within standard deviation of measurements taken on day 0, indicating that there was not a significant amount of degradation.

#### *Optimization of Printing Process*

A simple structure was designed in Solidworks to test the effects of print parameters on fidelity and resolution. The tested structure has a length and width of 6 mm, and a height of 0.6 mm, which is the print layer height (Figure 2). A single print layer structure was chosen, so that the printed structure could be imaged successfully in a single plane through tile scanning. A two-perimeter design was selected because these structures are small, thin, and prone to breaking, so this setting will make them more robust.

The ink flow rate, print speed, and infill percentage were the selected parameters to be tested because they directly influence the amount of ink being deposited at any given position in the test print and therefore must be optimized together. The ranges of each of these parameters were tested by printing test cubes and selecting the ranges of flow rate, print speed, and infill density values that generated prints

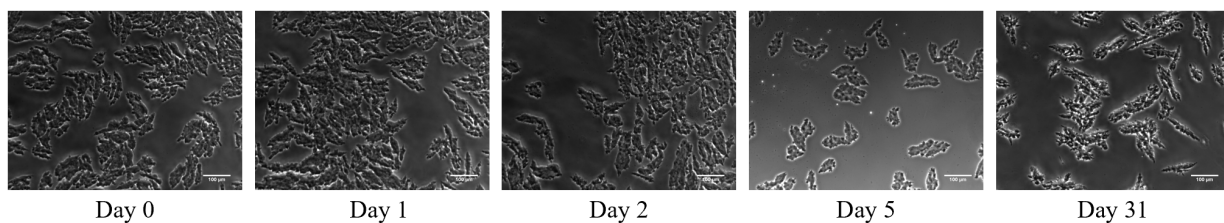


**Figure 1:** Support bath material on day 0, 1, 2, 5, and 31  
(Scale Bar Length = 100µm)

with defined features and would not fall apart. These ranges were 1 drop/2s to 1 drop/4s for flow rate, 10 mm/s to 14 mm/s for print speed, and 25-75% for infill percentage.

With this design, two replicates of test squares were 3D bioprinted using each combination of flow rates, print speeds, and infill percentages. These test squares were imaged as tile scans one day after printing (Figure 3). The printhead pressures used to

achieve the required flow rates for each print condition are listed in Table 1.

The test squares printed at 25% infill had greater porosity and less structural integrity during rinsing and handling than the higher density prints, while the test squares printed at 75% infill were more robust but less porous due to print lines merging before crosslinking. Each of the four densities tested may be advantageous in different applications depending on the

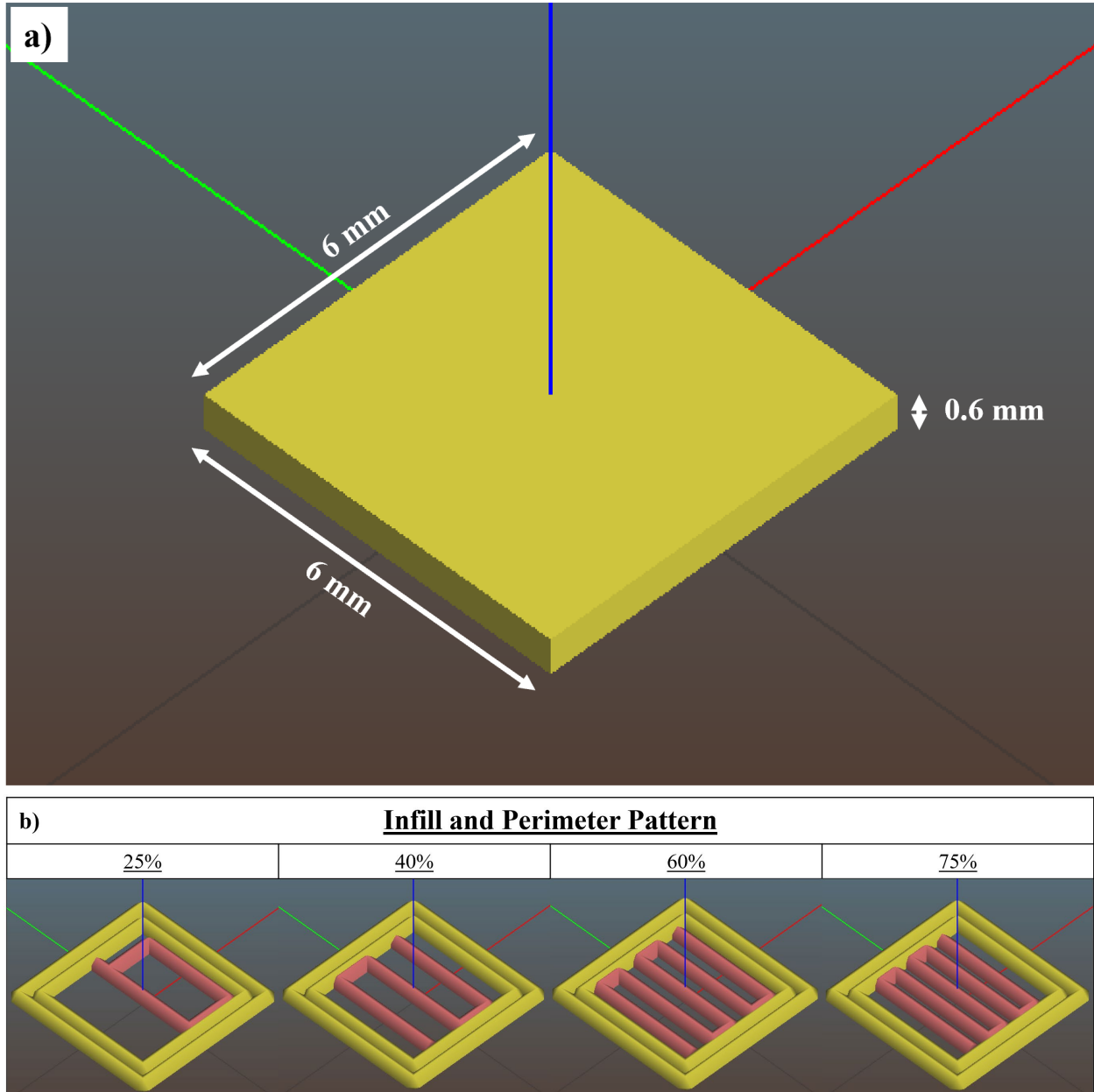


**Figure 2:** Test square design before and after print pattern was generated in Slic3r. (a) Test square design (6 mm x 6 mm x 0.6mm). (b) Slic3r generated two-perimeter print pattern with varied infill densities: 25%, 40%, 60%, 75%.

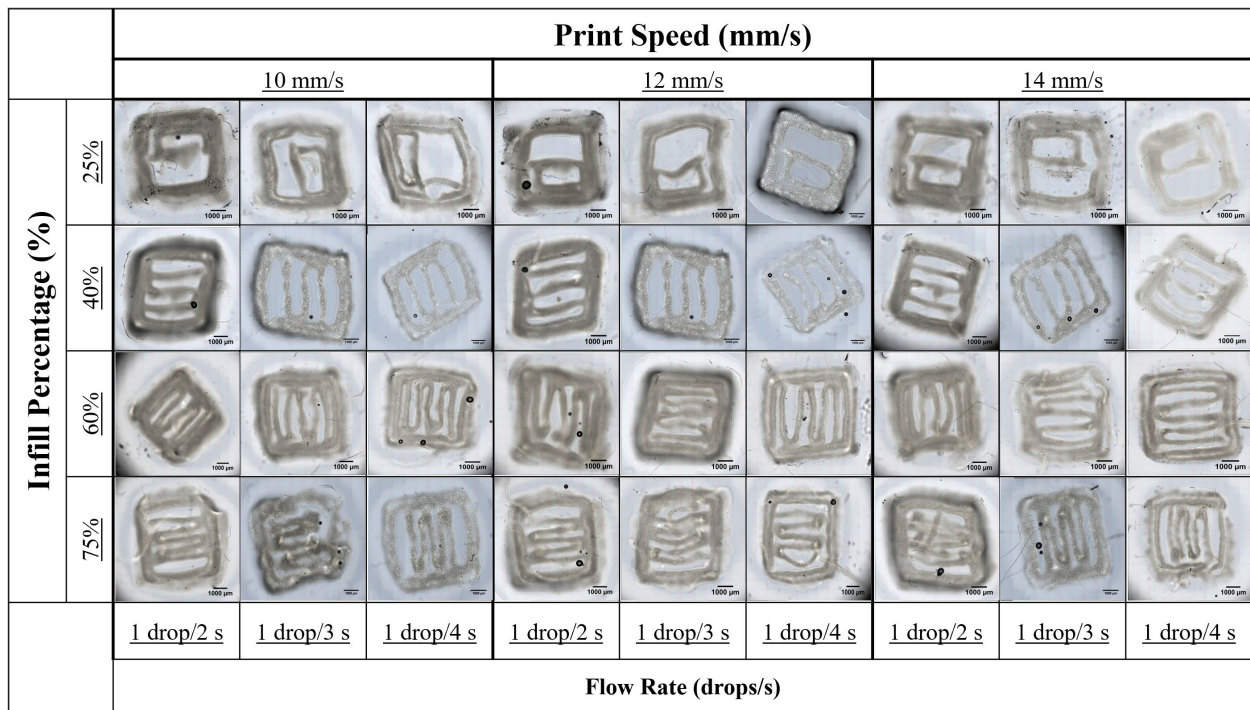


**Figure 3:** Tile scanned images of test prints. Flow rates (1 drop/2s, 1 drop/3s, 1 drop/4s), print speeds (10 mm/s, 12 mm/s, 14 mm/s), and infill densities (25%, 40%, 60%, 75%) were varied between prints. Scale Bar = 1000  $\mu$ m.

**Table 1:** Printhead pressures set to achieve required flow rates. Flow rates were set by adjusting the pressure of the pneumatic printhead and manually measuring the seconds between drops with a stopwatch. Set flow pressures were recorded for each flow rate and infill percentage and standard error between replicates was calculated. Printhead pressures were decreased to achieve an increase in flow rate.

Infill Percentage	Flow Rate		
	1 drop/2s	1 drop/3s	1 drop/4s
25%	36.5 $\pm$ 0.5 kPa	28.5 $\pm$ 1.5 kPa	25 $\pm$ 1 kPa
40%	36.5 $\pm$ 0.5 kPa	30.5 $\pm$ 1.5 kPa	26.5 $\pm$ 0.5 kPa
60%	37 $\pm$ 0 kPa	30 $\pm$ 3 kPa	26.5 $\pm$ 1.5 kPa
75%	35.5 $\pm$ 3.5 kPa	30 $\pm$ 2 kPa	27.5 $\pm$ 2.5 kPa

importance of strength and porosity.

Test square side length was selected as a measure of fidelity, or the ability for this printer to replicate a designed structure with this bioink. Infill line thickness was selected as a measure of resolution, or the smallest possible feature that can be printed by this printer with this ink. Test square side length and infill line thickness of each test print were measured using ImageJ for both replicates. Six

test square side lengths and three infill line thicknesses were averaged and plotted for each set of print parameters (Figures 4 and 5).

After plotting the test square side lengths as a function of each print condition, trends emerged between the measured side length and both the flow rate and print speed. Slower print speeds and faster flow rates resulted in longer side lengths, while the infill percentage seemed to have a negligible effect. Trends again also

## Test Square Side Length (mm) vs. Flow Rate (drops/s)

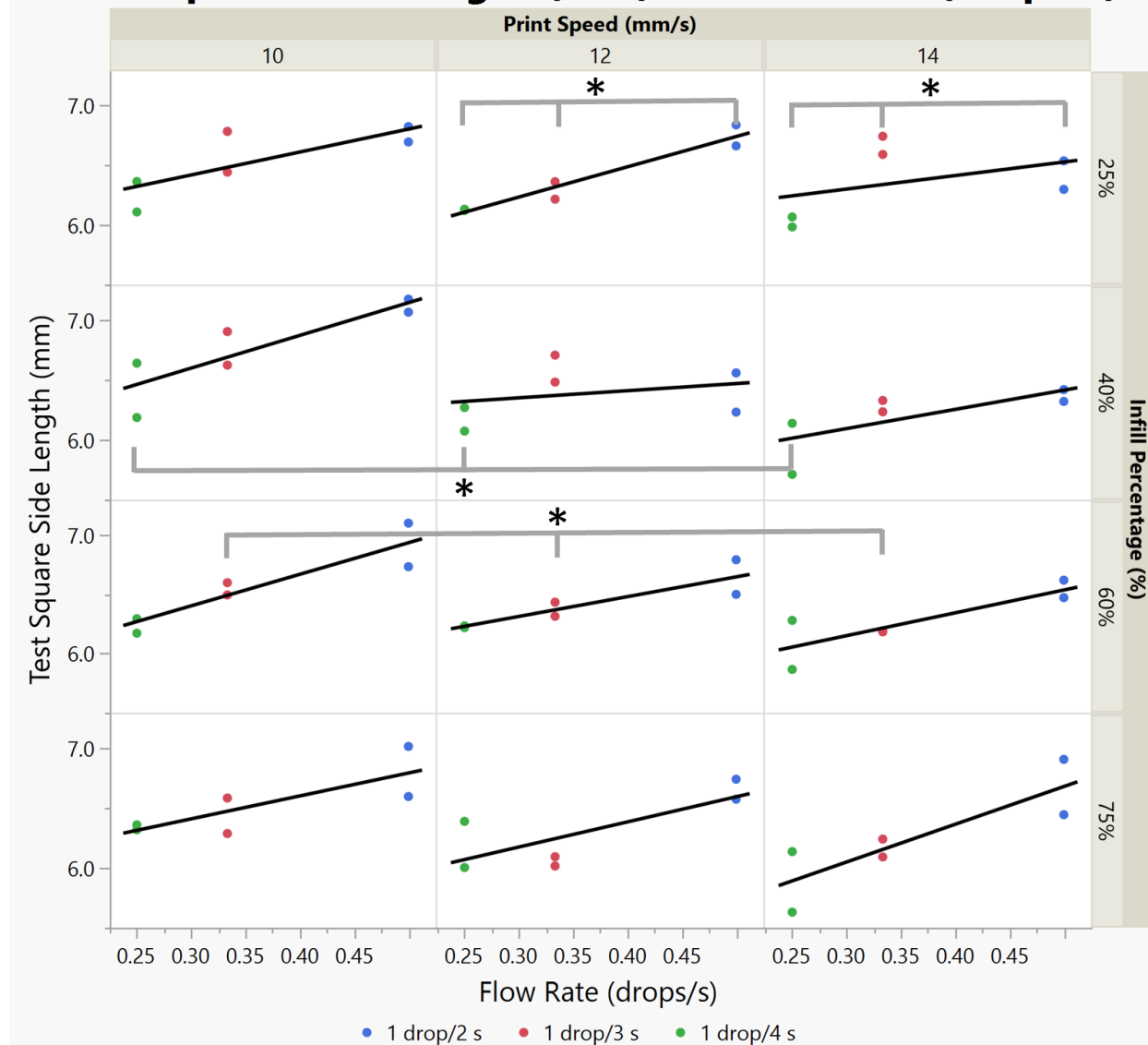


**Figure 4:** Test square side length measurements. Flow rates (1 drop/2s, 1 drop/3s, 1 drop/4s), infill densities (25%, 40%, 60%, 75%), and print speeds (10mm/s, 12mm/s, 14mm/s) were varied. The target side length set in the test square design was 6.0 mm. Most print conditions resulted in an oversized side length. Decreasing the print speed and increasing the flow rate resulted in an increased side length. Conditions with statistically significant trends are shown with an asterisk.

emerged between the infill line thickness and the flow rate, with slower print speeds and faster flow rates resulting in thicker infill lines; however, the trend in print speed was less pronounced. Increases in the infill percentage and print speed seem to result in a less pronounced effect of flow rate on the infill line thickness.

To summarize the effects of flow rate, print speed, and infill percentage and determine which parameters had a statistically significant effect on the test square side length and infill line thickness, the data within each print condition was pooled, and ANOVA tests were conducted for both measurements by each of the three print parameters tested (Figure 6) (Table 2).

## Infill Line Thickness (mm) vs. Flow Rate (drops/s)

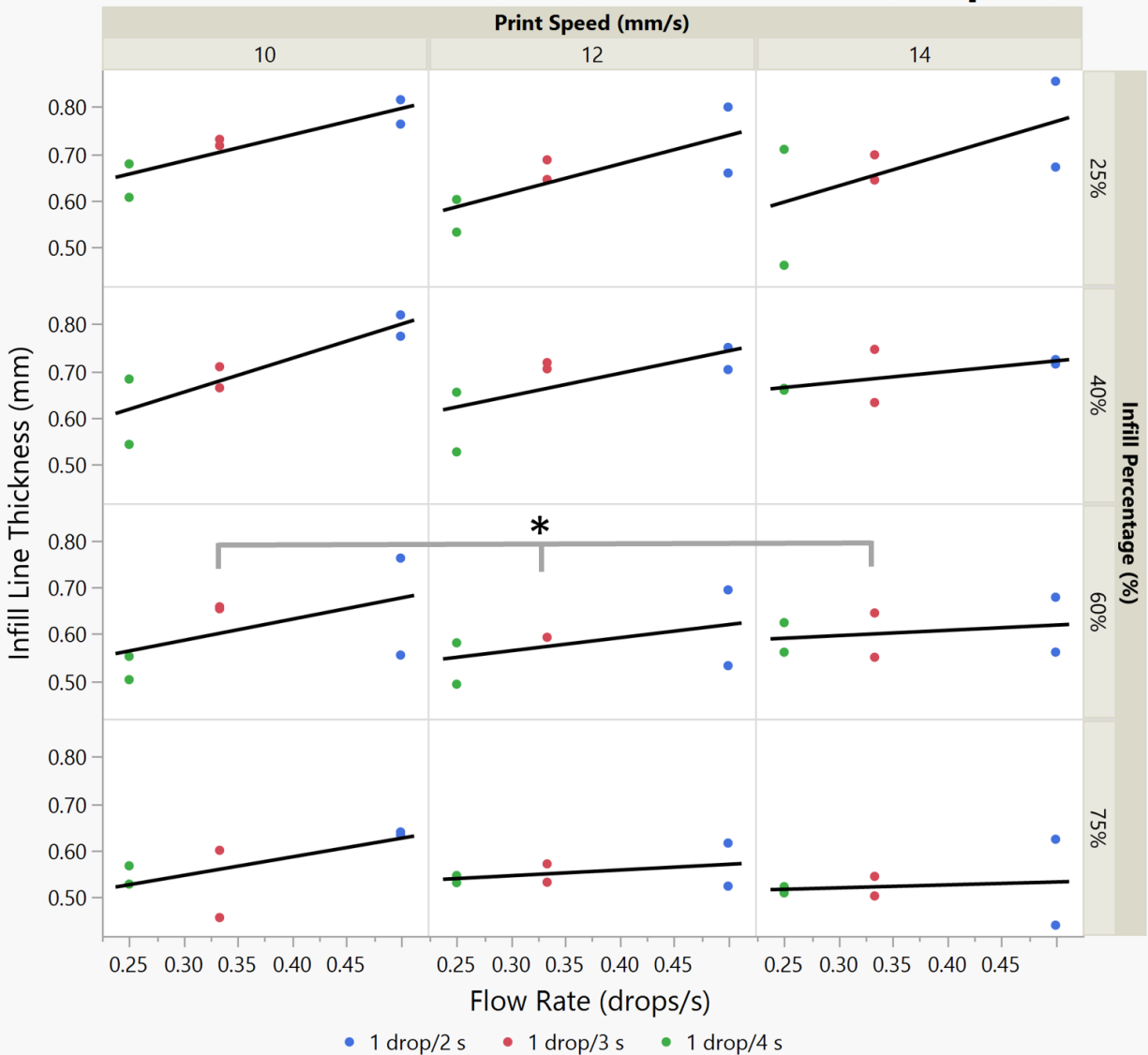


**Figure 5:** Infill line thickness measurements. Flow rates (1 drop/2s, 1 drop/3s, 1 drop/4s), infill densities (25%, 40%, 60%, 75%), and print speeds (10mm/s, 12mm/s, 14mm/s) were varied. The target infill line thickness set in the test square design was 0.6 mm. Decreasing the print speed and increasing the flow rate resulted in an increased infill line thickness. Conditions with statistically significant trends are shown with an asterisk.

From these tests, it was observed that an increase in flow rate results in a statistically significant decrease in both test square side length and infill line thickness, with p values of 0.0001 and 0.0004, respectively. Infill percentage did not have a statistically significant effect on the test square length; however, an increase in infill percentage resulted in a significant decrease in infill line

thickness. Inversely, an increase in print speed led to a statistically significant decrease in test square side length but did not have a significant effect on infill line thickness.

To determine whether these trends were consistent within each print condition, ANOVA tests were also conducted for each of the three print parameters, this time distinguishing by each combination of the other two print

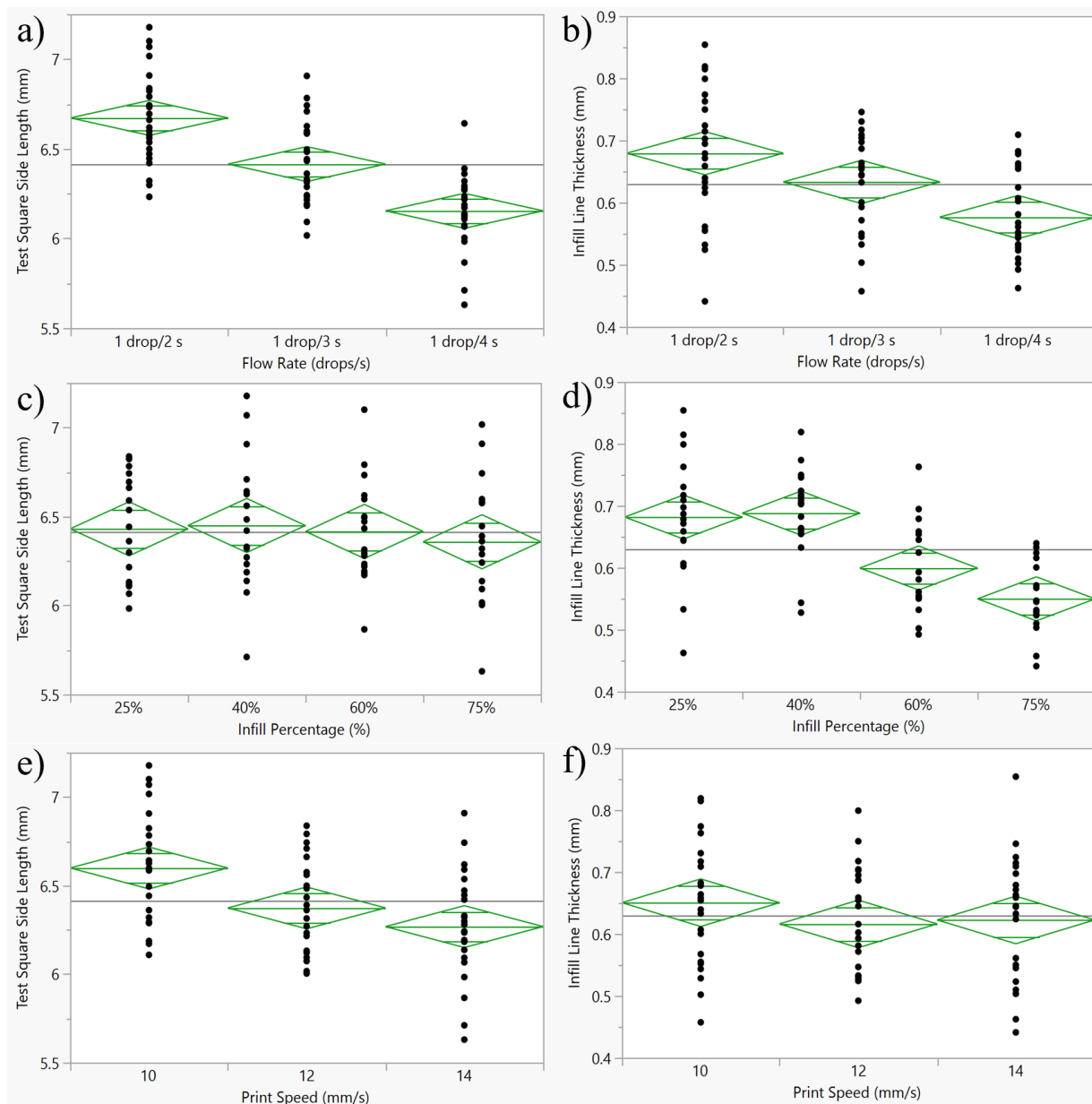


**Figure 6:** ANOVA test plots of pooled data for (a) test square side length by flow rate, (b) infill line thickness by flow rate (c) test square side length by infill percentage, (d) infill line thickness by infill percentage, (e) test square side length by print speed, and (f) infill line thickness by print speed

parameters (Table S1). Statistical significance ( $p < 0.05$ ) within conditions were denoted in Figure 5 with asterisks.

Because infill percentage chosen for 3D bioprinting may change depending on porosity and robustness requirements of prints, the test square side length data and infill line thickness data from each infill condition were pooled for each set of flow rates and print speeds to define an optimal set of print parameters regardless of

the application (Figure 7a-b). The normalized fidelity for each condition was then calculated as a percentage of the designed side length dimension by dividing the test square side length values by 6 mm (Figure 7c). Similarly, the normalized resolution at each combination of flow rates was calculated as a percentage of the designed infill line thickness by dividing the infill line thickness values by 0.6 mm (defined by the printhead needle inner diameter) (Figure 7d).

**Table 2:** P-values from ANOVA tests of pooled data for each print parameter.

\*denotes statistical significance ( $p < 0.05$ )

ANOVA Test Factor	Test Square Side Length	Infill Line Thickness
Flow Rate	0.0001*	0.0004*
Infill Percentage	0.8472	0.0001*
Print Speed	0.0007*	0.4125

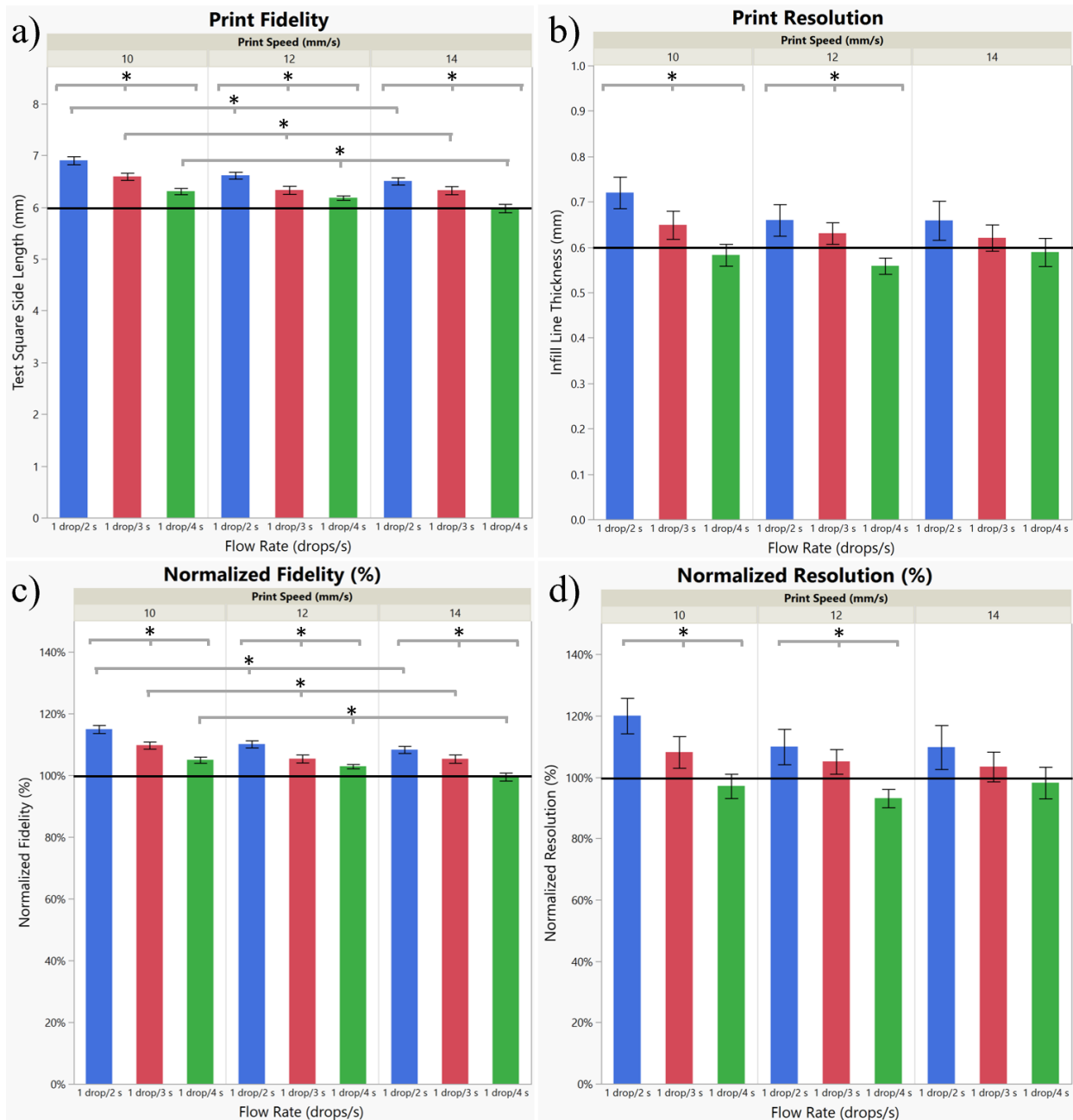


**Figure 7:** Test print fidelity and resolution. (a) Fidelity of test prints. (b) Resolution of test prints. (c) Normalized fidelity of test prints. (d) Normalized resolution. Conditions with statistically significant trends are shown with an asterisk.

The majority of print conditions tested resulted in prints with both normalized resolutions and fidelities above 100%. Decreasing the flow rate and increasing the print speed brought both the normalized fidelity and normalized resolution closer to 100%. One print condition, a flow rate of 1 drop/4s with a print speed of 14 mm/s, resulted in a normalized fidelity within standard error of 100% of the side length. Three print conditions, a flow rate of 1 drop/4s with a print speed of 10mm/s, a flow rate of 1 drop/3s with a print speed of 14 mm/s, and a flow rate of 1 drop/4s with a print speed of 14 mm/s, brought the normalized resolution within standard error of 100% of the infill line thickness.

## Discussion

While great strides have been made towards developing 3D-bioprinted, patient-specific, cell-laden organ models, many challenges still exist including print resolution, fidelity, reproducibility, and cell viability. When printing with hiPSC-CMs, the optimization of these conditions is particularly important because the maturation of these cells is highly dependent on their environment. This study addresses many of these key challenges by establishing a straightforward methodology for quantifying and assessing trends in resolution and fidelity of 3D-bioprinted structures printed under a variety of conditions.

### *Establishing a Methodology for Quantifying Resolution and Fidelity*

Without the ability to produce 3D structures accurately and consistently through 3D printing, generating and improving organ models and other structures cannot be

successful. Using a simple square geometry designed in Solidworks, a straightforward and relatively quick methodology was developed for assessing the resolution and fidelity of 3D printed structures with a low viscosity bioink. Through design iterations and testing, it was determined that a 6 mm x 6 mm x 0.6 mm structure should be used to print, image, and analyze a set of bioprinting parameters. The designed Solidworks file was processed using Slic3r software for 3D bioprinting using two perimeters. These design choices enable the generation of a structurally robust print that allows for visualization of changes in infill density, flow rate, and print speed. Using this methodology, the resolution and fidelity of the test structure were assessed for the bioprinting parameters of flow rate, print speed, and infill density. As whole structures are created by printing perimeter and infill lines in 3D printing, the resolution was quantified by comparing the measured thickness of a single line of infill to the theoretical line thickness. This theoretical line thickness was estimated to be the inner diameter of the printhead needle and was established in the Slic3r settings. The fidelity of the prints was determined by comparing the measured side length of the square prints to the designed side length value, which was established in the test cube design to be 6 mm. Using these methods, both resolution and fidelity were quantified both as measured values and as a percentage of the designed values. Applying a quantitative methodology for assessing bioprinting success in this way is critical to improving the functionality and reproducibility of 3D bioprinted models.

### *Determination of the Resolution and Fidelity of 3D Bioprinting Parameters*

Using the established methodology outlined previously, the resolution and fidelity of both the overall structure and a single print line were determined for a range of flow rates, print speeds, and infill densities. It was observed that faster print speed and slower flow rates resulted in prints with finer resolution and improved fidelity, sometimes at the expense of structural integrity depending on the infill percentage. These trends should be further investigated, however, in order to establish statistical significance. Based on these results, the best conditions for both fidelity and resolution were a print speed of 14 mm/s at a flow rate of 1 drop/4s and a print speed of 12 mm/s at a flow rate of 1 drop/4s, and the worst condition for both the fidelity and resolution was a print speed of 10 mm/s at a flow rate of 1 drop/2s. These conditions differ from those currently used to print cardiac organoid models (print speed of 10 mm/s and a flow rate of 1 drop/3s)<sup>5</sup> and should be considered as a starting point for implementation in 3D bioprinting protocols using low viscosity bioinks.

### *Future Considerations*

To fully assess the effect of these printing parameters, further research is required. A limitation to this method is the inability to measure the height or z-resolution of the prints. As the height of the structure will depend on the spreading of the low-viscosity ink in the x- and y-dimensions, the method detailed in this study should give a sufficient approximation of overall print resolution and fidelity, but it would be beneficial moving forward to ensure the height of the structure is similar to the designed height.

Furthermore, the improved parameters suggested here should be applied to more complex shapes, such as the hChaMP.5. Because of the more irregular shape of organic geometries, it is hypothesized that the infill density will be less homogenous throughout the structure, which may affect the spatial fidelity, porosity, and structural integrity of the final print. While there was not a large effect from the infill density on the resolution and fidelity in this study, the infill density may have more of an effect on an irregular structure depending on the method by which the Slic3r software generates infill patterns. Lastly, the cell viability of structures 3D bioprinted with each set of printing conditions should also be assessed in future works. As shear stress is known to influence cell viability,<sup>6,7</sup> some conditions proposed here may not be optimal for printing with cells, even if it improves the resolution and fidelity of the final printed structure.

### **Conclusion**

In this work, a methodology was developed to quantify and assess trends in both the print fidelity and resolution associated with varying print parameters. These outcomes will be used to inform future work in assessing the resolution and fidelity of 3D bioprinting complex organic structures with low-viscosity inks and the cell viability of 3D bioprinted structures generated with varying print parameters. Once an optimal methodology and set of 3D bioprinting conditions for resolution, fidelity, and cell viability is determined, it can be used for the development of 3D printed organ models to support the future of regenerative medicine and disease modeling.

## Acknowledgements

We would like to thank Anthony Baker and Jeffrey Ai for their work in optimizing the support bath material.

## References

- 1) L. A. MacQueen, S. P. Sheehy, C. O. Chantre, J. F. Zimmerman, F. S. Pasqualini, X. Liu, J. A. Goss, P. H. Campbell, G. M. Gonzalez, S. J. Park, A. K. Capulli, J. P. Ferrier, T. F. Kosar, L. Mahadevan, W. T. Pu, K. K. Parker, "A tissue-engineered scale model of the heart ventricle." *Nature Biomedical Engineering*. 23 Jul 2018, 2(12):930-941. 10.1038/s41551-018-0271-5.
- 2) T. J. Hinton, Q. Jallerat, R. N. Palcheski, J. H. Park, M. S. Grodzicki, H. Shue, M. H. Ramadan, A. R. Hudson, A. W. Feinberg, "Three-dimensional printing of complex biological structures by freeform reversible embedding of suspended hydrogels." *Science Advances*. 23 Oct 2015, 1(9):e1500758. 10.1126/sciadv.1500758.
- 3) A. Lee, A. R. Hudson, D. J. Shiwerski, J. W. Tashman, T. J. Hinton, S. Yerneni, J. M. Bliley, P. G. Campbell, A. W. Feinberg, "3D bioprinting of collagen to rebuild components of the human heart." *Science*. 02 Aug 2019, 365(6452):482-487. 10.1126/science.aav9051.
- 4) M. E. Kupfer, W. Lin, V. Ravikumar, K. Qiu, L. Wang, Li. Gao, D. B. Bhuiyan, M. Lenz, J. Ai, D. Townsend, J. Zhang, M. C. McAlpine, E. G. Tolkacheva, B. M. Ogle, "In situ expansion, differentiation and electromechanical coupling of human cardiac muscle in a 3D bioprinted, chambered organoid." *Circulation Research*. 31 Mar 2020, 127:207-224. 10.1161/CIRCRESAHA.119.316155.
- 5) E. Mirdamadi, J. W. Tashman, D. J. Shiwerski, R. N. Palchesko, A. W. Feinberg, "FRESH 3D Bioprinting a Full-Size Model of the Human Heart." *ACS Biomater. Sci. Eng*. 23 Oct 2020, 6(11):6453-6459. 10.1021/acsbiomaterials.0c01133.
- 6) G. Gillispie, P. Prim, J. Copus, J. Fisher, A. G. Mikos, J. J. Yoo, A. Atala, S. J. Lee, "Assessment Methodologies for Extrusion-Based Bioink Printability." *Biofabrication*. 29 Feb 2020, 12(2):022003. 10.1088/1758-5090/ab6f0d.
- 7) P. Machiraju, S. C. Greenway, "Current methods for the maturation of induced pluripotent stem cell-derived cardiomyocytes." *World J Stem Cells*. 26 Jan 2019, 11(1):33-43. 10.4252/wjsc.v11.i1.33.